



**HAL**  
open science

# Antiparallel magnetic merging signatures during IMF BY»0: longitudinal and latitudinal cusp aurora bifurcations

S. Massetti

► **To cite this version:**

S. Massetti. Antiparallel magnetic merging signatures during IMF BY»0: longitudinal and latitudinal cusp aurora bifurcations. *Annales Geophysicae*, 2006, 24 (8), pp.2299-2311. hal-00318161

**HAL Id: hal-00318161**

**<https://hal.science/hal-00318161>**

Submitted on 18 Jun 2008

**HAL** is a multi-disciplinary open access archive for the deposit and dissemination of scientific research documents, whether they are published or not. The documents may come from teaching and research institutions in France or abroad, or from public or private research centers.

L'archive ouverte pluridisciplinaire **HAL**, est destinée au dépôt et à la diffusion de documents scientifiques de niveau recherche, publiés ou non, émanant des établissements d'enseignement et de recherche français ou étrangers, des laboratoires publics ou privés.

# Antiparallel magnetic merging signatures during IMF $B_Y \gg 0$ : longitudinal and latitudinal cusp aurora bifurcations

S. Massetti

Istituto di Fisica dello Spazio Interplanetario IFSI-INAF, Italy

Received: 24 March 2006 – Revised: 13 June 2006 – Accepted: 17 July 2006 – Published: 13 September 2006

**Abstract.** A prominent dayside auroral event, occurred during an IMF  $B_Y$ -dominated time interval, and characterized by the contemporaneous longitudinal and latitudinal cusp bifurcations, is reported. The event was recorded the 19 December 2002, between about 09:30–10:45 UT, by the ITACA<sup>2</sup> twin auroral monitors system, in the Greenland-Svalbard zone. The splitting of the ionospheric footprint of the geomagnetic cusp, traced by the dayside auroral activity, was recently identified with the signatures of antiparallel reconnection episodes ongoing at different magnetopause locations, during large IMF  $B_Y$  periods. The first part of the event showed a broad longitudinal bifurcation of the red-dominated cusp aurora, displaced in the prenoon and postnoon, with a separation up to  $\sim 1800$  km, during northeast directed IMF (clock-angle rotating from  $45^\circ$  to  $90^\circ$ ). This observation widens the range of IMF regimes that are known to drive a longitudinal bifurcation of the cusp, since previous case-studies reported these events to occur during southeast/southwest oriented IMF (clock-angle  $\approx 135^\circ$ ). The second part of the event, developed when the IMF turned to a nearly horizontal orientation ( $B_Y \gg 0$ ,  $B_Z \sim 0$ , clock-angle  $\sim 90^\circ$ ), and exhibited the simultaneous activation of the cusp auroras in three distinct areas: i) two of them associated to the above-mentioned longitudinally bifurcated cusp ( $\sim 73^\circ$ – $75^\circ$  CGM latitude, type 1 cusp aurora), and linked to (near)antiparallel magnetic reconnection patches equatorward the northern and the southern cusp, ii) the other one characterized by isolated high-latitude ( $\sim 76^\circ$ – $77^\circ$  CGM latitude, type 2 cusp aurora) rayed arc(s) with intense green emission, and triggered by (near)antiparallel merging at the northern lobe (usually observed during positive IMF  $B_Z$ ), poleward the local cusp. During this phase, the longitudinal separation of the low-latitude type 1 cusp aurora was about 1000 km wide, with a 500 km gap, while the latitudinal

separation between low- (type 1) and high-latitude (type 2) cusp auroras, in the postnoon, was about 270–280 km at its maximum. The longitudinal gap, corresponding to a zone with weak auroral emission, was found to likely map to the component reconnection region at the subsolar magnetopause. The magnetic merging topology that can be drawn on the basis of the reported cusp auroras support the idea of a “mixed” merging scheme, with (near)antiparallel reconnection at high-latitudes, and component reconnection in the subsolar region, as recently proposed by other authors.

**Keywords.** Magnetospheric physics (Solar wind-magnetosphere interactions) – Ionosphere (Ionosphere-magnetosphere interactions) – Space plasma physics (Magnetic reconnection)

## 1 Introduction

It is well-known that the solar wind – magnetosphere – ionosphere coupling on the dayside can be schematically outlined in terms of the IMF  $B_Z$  component. When this parameter is negative, the magnetic reconnection is favored and occurs at low-latitudes, equatorward the geomagnetic cusps. On the contrary, when the IMF  $B_Z$  is positive, the magnetic merging is confined on the geomagnetic lobes (high-latitudes), poleward each cusp. More generally, the presence of a non-zero IMF  $B_Y$  component leads to intermediate reconnection topologies, which can be conveniently categorized by means of the so-called IMF clock-angle, defined as follow:

$$\begin{aligned} \theta &= \tan^{-1} (|B_Y|/B_Z) & \text{for } B_Z > 0 \\ \theta &= \pi - \tan^{-1} (|B_Y/B_Z|) & \text{for } B_Z < 0 \end{aligned} \quad (1)$$

The clock-angle is maximum ( $180^\circ$ ), when  $B_Z < 0$  and  $B_Y = 0$ , is equal to  $90^\circ$ , when  $B_Z = 0$  and  $B_Y \neq 0$ , and reduces to zero, when  $B_Z > 0$  and  $B_Y = 0$ . In the recent past, there has been an increasing interest in the study of the response of the

Correspondence to: S. Massetti  
(stefano.massetti@ifsi-roma.inaf.it)

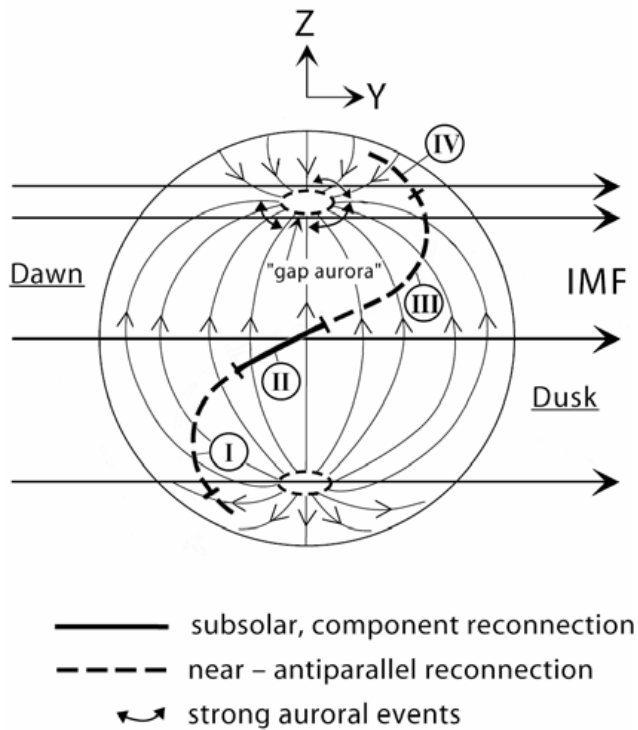


**Fig. 1.** Sketch of the dayside merging topology for a horizontal IMF (clock-angle =  $90^\circ$ ), on the basis of the results of Moore et al. (2002), drawn by adapting the original figure in Sandholt et al. (2004). Component (II) and (near)antiparallel merging regions (I, III, IV) are evidenced, together with the associated dayside aurora signatures mapping to the northern cusp.

magnetospheric-ionospheric system during periods that are characterized by a significant horizontal IMF component, that is,  $|B_Y/B_Z| > 1$ , or even  $\gg 1$  ( $\theta \sim 90^\circ$ ). See, for example, McCrea et al. (2000); Maynard et al. (2002); Němeček et al. (2003); Sandholt and Farrugia (2003); Sandholt et al. (2004); Trattner et al. (2005); Massetti (2005).

The magnetic merging topologies and the related ionospheric signatures, under the effect of a significant IMF  $B_Y$  component, vary substantially among the different reconnection theories: the antiparallel reconnection model (e.g.: Crooker, 1979; Luhmann et al., 1984), the component reconnection model (e.g. Cowley, 1976; Cowley and Owen, 1989), and the “mixed” reconnection model (Moore et al., 2002; Sandholt et al., 2004). Following the first theory, magnetic merging can occur only where the magnetosheath and magnetospheric fields are antiparallel, or nearly antiparallel (high-shear regime), a condition that is satisfied in the high northern/southern latitudes in the postnoon/prenoon sector, for positive IMF  $B_Y$ , and vice versa for negative IMF  $B_Y$ . In this case, no merging is present in the subsolar region. On the contrary, for the component reconnection theory there is no such a stringent condition, and the magnetic merging

can take place between fields with any orientation, along a tilted X-line that cross the subsolar region, approximately rotated by  $\theta/2$  with respect to the equatorial plane. Finally, the “mixed” model states the merging takes place along an S-shaped X-line that crosses the subsolar region and wraps around the cusps, and can be viewed as a superimposition of component reconnection, at lower latitudes, and antiparallel reconnection, at higher latitudes (see Figs. 2 and 4 in Moore et al., 2002). Figure 1 shows a sketch of the dayside merging topology during a horizontal IMF ( $B_Y > 0$ , and  $B_Z = 0$ ) according to the results of Moore et al. (2002), drawn by adapting the original figure (Fig. 25) in Sandholt et al. (2004). In the high-latitude Northern Hemisphere, the effect of the antiparallel reconnection is to produce three distinct ionospheric signatures: two of them are linked to reconnection patches equatorward the southern and the northern cusps, occurring at different magnetic local time in the two hemispheres (marked as I, and III), while the third one is connected to magnetic merging poleward the local northern cusp (marked as IV).

The spatial separation between the merging regions I and III produces a split of the cusp, often referred as “longitudinal cusp bifurcation”, because the northern and southern cusp footprints are shifted away from the magnetic noon (in opposite directions), due to the non-zero IMF  $B_Y$ -component. When  $B_Y$  is positive, the northern longitudinally bifurcated cusp is composed of the local (main) cusp, displaced in the postnoon, and a prenoon footprint magnetically conjugated to the reconnection region near (equatorward) the southern cusp. The gap, between the footprints of regions I and III, corresponds to the subsolar component reconnection region (marked as II); here the magnetic merging is progressively less effective as the IMF clock-angle decreases, with a possible cutoff below  $40^\circ$ – $50^\circ$  (Gosling et al., 1982, 1990; Phan and Paschmann, 1996). An interesting feature of the “mixed” model is that the merging region II, and the resulting gap aurora, is noticeably shifted in the prenoon (Sandholt et al., 2004).

A second kind of cusp splitting arises from the spatial separation between the merging regions III and IV, due to the simultaneous merging equatorward the local cusp and poleward of it (latitudinal cusp bifurcation). The latter is often termed “lobe reconnection”, and is typically observed during northward IMF, but there are observational evidences that it can also take place during IMF  $B_Y$ -dominated time intervals (e.g.: McCrea et al., 2000; Sandholt et al., 2001).

The dayside (cusp) auroras are a unique tool to track the large-scale reconnection process taking place at the dayside magnetopause, and the analysis of both ground- and space-based auroral observations can provide important information on the merging topologies. Although the relatively small field-of-view of a single ground-based imager, with respect to the ionospheric cusp footprint extension, and/or the low spatial and temporal resolution of the space-based instruments can constitute an obstacle, particularly during IMF

$B_Y$ -dominated periods, when the cusp aurora activity spreads considerably in longitude.

In this work, we analyze a remarkable dayside auroral event that took place the 19 December 2002, between 09:30–10:45 UT. It was recorded by the ITACA<sup>2</sup> twin all-sky cameras system, devoted to the high-latitude auroral imaging, in the Greenland-Svalbard sector. The wide field-of-view of ITACA<sup>2</sup> allows to observe a broad zone in the high-latitude ionosphere, and hence to perform a comparison between ground-recordings and space-based data. The event key-features are: i) a wide longitudinal cusp bifurcation during north-east directed IMF, ii) the contemporaneous occurrence of longitudinal and latitudinal cusp bifurcations, during horizontal IMF condition (that is:  $|B_Y| \gg 0$  and  $B_Z \sim 0$ ).

In the following section (Sect. 2), a brief description of the datasets used in the analysis, is given. In Sect. 3, the cusp aurora activity is discussed in relation to the magnetic merging topologies, as a function of the IMF clock-angle, as follows: longitudinal cusp bifurcation ( $45^\circ \leq \theta \leq 90^\circ$ , Sect. 3.1), latitudinal cusp bifurcation ( $\theta \simeq 90^\circ$ , Sect. 3.2), and auroral dynamics during horizontal IMF ( $\theta \simeq 90^\circ$ , Sect. 3.3). A comparison with the observations obtained by the FUV instruments onboard the IMAGE satellite is then reported in Sect. 4, while the conclusions are summarized in Sect. 5.

## 2 Datasets

This study is based on the analysis of the dayside auroral event occurred 19 December 2002, between 09:30–10:45 UT. The following datasets were used:

- Ground-based red- and green-line (630.0 nm, 557.7 nm) aurora images from the ITACA<sup>2</sup> all-sky camera database (IFSI-INAF, PNRA). The all-sky images recorded by the two ITACA<sup>2</sup> stations, located at the Svalbard (ITACA-NAL, Ny-Ålesund, 78.92° N, 11.93° E), and on the east coast of Greenland (ITACA-DNB, Daneborg, 74.30° N, 20.22° W), were combined to obtain a resulting field-of-view of about 20° MLAT × 135° MLON (i.e.: about 09:00 MLT), centered at about 75.5° of magnetic latitude;
- Space-based far ultraviolet auroral images obtained by the WIC (Wide-Band Imaging Camera, 140–180 nm), SI12, and SI13 (Spectrographic Imager, 121.82 nm and 135.6 nm) IMAGE-FUV imagers, on-board the IMAGE satellite (Imager for Magnetopause-to-Aurora Global Exploration);
- Spectrograms from the DMSP F13 (09:10–09:13 UT, and 10:40–10:56 UT), F14 (10:39–10:44 UT), and F15 (09:38–09:43 UT) satellite transits, were used to categorize the particle precipitation region within the ITACA<sup>2</sup> field-of-view, thanks to the automated region identification algorithm (JHU/APL);

- Plasma and magnetic field data obtained by the CPI and MGF instruments onboard the Geotail satellite (NASA Goddard Space Flight Center dataset), were employed to inspect the solar wind conditions during the developing of the auroral event. Geotail was located on the Earth's dawn side at about  $X_{GSE}=8 R_E$ ,  $Y_{GSE}=-27 R_E$ , and  $Z_{GSE}=5 R_E$ , and the approximate time delay between the satellite data and the ionospheric signatures was estimated to be about 10 min in the period  $\approx 10:00$ – $10:45$  UT, by summing the propagation time from satellite to Earth's magnetopause ( $\Delta_{S-MP} \approx 5$  min), and from magnetopause to ionosphere ( $\Delta_{MP-IO} \approx 2$ – $3$  min), and by taking into account the 110 s mean lifetime associated to the 630.0 nm red auroral emission (at 400 km of altitude).

## 3 Dayside auroral activity

The 19 December 2002 dayside event was recently discussed by the author (Massetti, 2005) from the point of view of the quasi-periodic cusp aurora activations, and the correlated ULF Pc5 ground magnetic variations, which occurred during the prolonged period of stable horizontal IMF ( $\theta \sim 90^\circ$ ). The magnetic pulsations were found to be shaped as a train of traveling convection vortices (TCVs), developing close to the prenoon convection reversal boundary, and moving anti-sunward in phase with the transit of the auroral forms. That activity was found to have several aspects in common with quasi-periodic TCV events described by Clauer and coworkers (e.g.: Clauer, 2002, and references therein), observed under the same IMF condition ( $\theta \sim 90^\circ$ ).

In this paper, we focus our attention to the simultaneous longitudinal and latitudinal cusp aurora bifurcations, and on the magnetic reconnection topology that can be inferred from the observed dayside aurora activity. Figure 2 reports the temporal trend of the interplanetary parameters:  $V_{SW}$ ,  $P_{dyn}$ , IMF  $B_X$ , IMF  $B_Y$ , IMF  $B_Z$  and the clock-angle  $\theta$  (Eq. 1), in the time interval 08:50–11:00 UT. All the parameters are plotted with an estimated time lag of +10 minutes (see Sect. 2). The transit of the F13, F14 and F15 DMSP satellites across the ITACA<sup>2</sup> field-of-view (Sect. 2) are indicated on the x-axis (arrows), while a supplementary x-axis shows the magnetic local time in Ny-Ålesund (MLT=UT+3:10). The shaded areas indicate two close periods with almost steady horizontal IMF ( $\theta \sim 90^\circ$ ).

In the following, the event is discussed by subdividing the time period into three contiguous intervals, characterized by a smooth IMF rotation from northward to eastward, according to the IMF clock-angle  $\theta$  regime:

- 09:00–09:27 UT, clock-angle  $0^\circ \leq \theta \leq 45^\circ$ ;
- 09:28–09:54 UT, clock-angle  $45^\circ \leq \theta \leq 90^\circ$ ;
- 09:55–10:45 UT, clock-angle  $\theta \simeq 90^\circ$ .

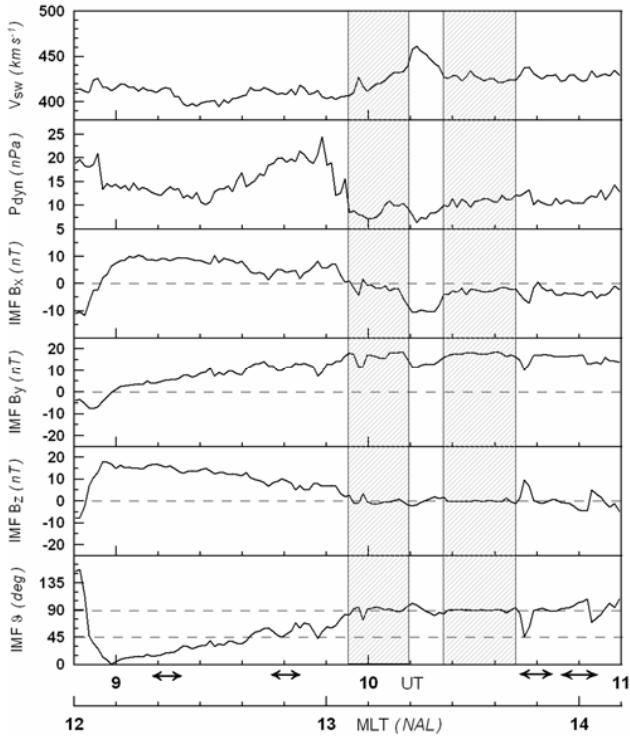


**Fig. 2.** Solar wind parameters derived from the Geotail data, plotted with a +10 min shift. The shaded areas mark the two periods (about 09:56–10:09 UT, and 10:19–10:33 UT) with almost steady clock-angle  $\sim 90^\circ$ . These two periods are separated by a discontinuity in the solar wind. The four segments below the x-axis indicate the transit of the DMSP satellites.

### 3.1 Longitudinal cusp bifurcation during IMF clock-angle $\approx 45^\circ$ – $90^\circ$

We start the discussion from the abrupt  $180^\circ$  rotation of the IMF occurred between 08:50–09:00 UT, when all the IMF components turned from negative to positive. In particular, the IMF  $B_X$  and  $B_Z$  underwent a sharp inversion, reaching about +10 nT, and +18 nT, respectively (Fig. 2). Few minutes later (09:08 UT), an intense red aurora spot emerged south of the Svalbard archipelago close to the local magnetic noon, at about  $72^\circ$ – $74^\circ$  MLAT, that is, about two degrees below to the expected cusp location ( $\sim 75.5^\circ$ – $76.0^\circ$  MLAT). This displacement was likely due to the unusually high solar wind dynamic pressure ( $\sim 12$ – $14$  nPa) (e.g.: Newell and Meng, 1992). That sudden activation of the cusp aurora is analogous to the one reported by Sandholt et al. (2000), after a sharp turning of both IMF  $B_X$  and  $B_Z$  to positive values ( $\sim 10$  nT). Between 09:08–09:27 UT, as the IMF clock-angle rotated from about  $10^\circ$  to  $45^\circ$ , the cusp aurora gradually expanded longitudinally reaching a maximum extension of  $40^\circ$ – $50^\circ$ , at 09:22 UT, while some green rayed emission appeared at its poleward boundary.

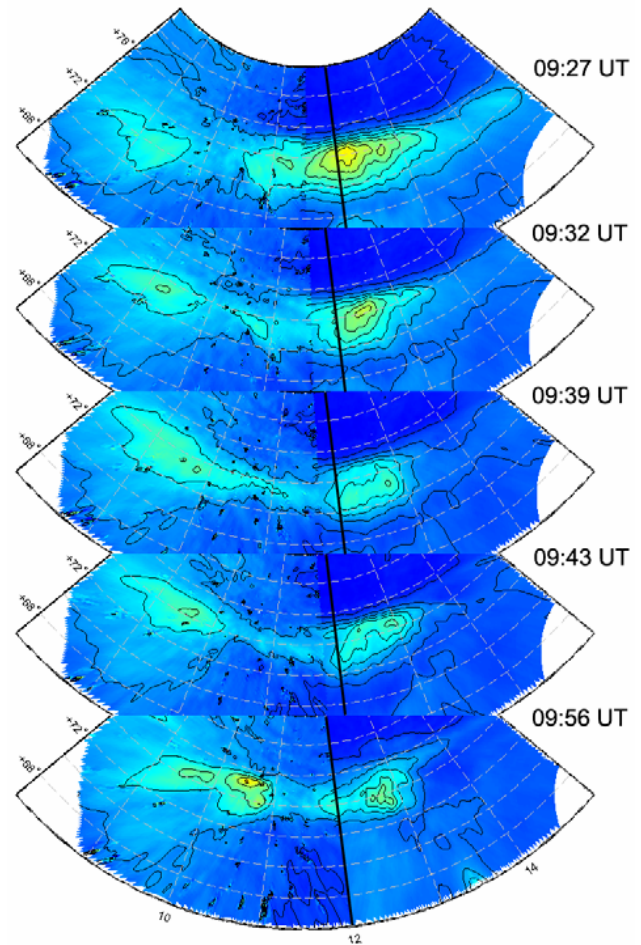


**Fig. 3.** A time-sequence illustrating the development of the longitudinal cusp bifurcation, as recorded by ITACA<sup>2</sup> monitors, between 09:27–09:56 UT. The original all-sky images were mapped to 400 km of altitude, using AACGM coordinates. The local (northern) cusp ionospheric footprint is clearly visible in the top panel, centered at about 12:00 MLT,  $73.5^\circ$  MLAT. The cusp gradually bifurcates longitudinally as the IMF clock-angle rotated from about  $45^\circ$  to  $90^\circ$ , between 09:28–09:56 UT. The longitudinal separation was about 1800 km, at the beginning of the sequence, while it reduced to about 1200 km when  $\theta$  approaches  $90^\circ$  (see Table 1). The gap was maximum ( $\sim 1100$  km) for  $\theta \sim 45^\circ$ – $50^\circ$ , and minimum ( $\sim 550$  km) for  $\theta \sim 90^\circ$ . Between 09:43–09:56, an abrupt change occurred in the solar wind dynamic pressure (Fig. 2). The solid lines mark the magnetic noon (12:00 MLT).

As the IMF clock-angle approached  $45^\circ$ , a second cusp aurora spot appeared above the east coast of Greenland, at about 09:30 MLT, and  $72^\circ$  MLAT. Figure 3 shows the map projection of the red aurora emission obtained by merging the all-sky camera images taken from both ITACA-NAL (Svalbard) and ITACA-DNB (Greenland). By comparing the all-sky images recorded by the two monitors, the 630.0 nm peak emission height was estimated to be in the range 350–400 km. This relatively high value is typical for the red-dominated

dayside cusp auroras, which are mainly induced by soft electron precipitation (e.g., Lockwood et al., 1993, 2000). On the base of the peak emission height it is also possible to derive a rough estimation of the energy of the incoming electron, which, for 350–400 km, corresponds to about 100–200 eV (Millward et al., 1999). That energy range fit with the measurements of the DMPS satellites, along the ITACA<sup>2</sup> field-of-view.

The five panels of Fig. 3 illustrate the evolution of the cusp aurora emission in the time interval 09:27–09:56 UT, while the IMF clock-angle rotated from 45° to 90°. Starting from 09:27 UT (top panel), the postnoon footprint (on the right) contracted, and a longitudinal bifurcation clearly developed after 09:32 UT. At the beginning of the sequence, the separation between the centers (roughly matching the 630.0 nm emission maxima) of the two cusp spots, was roughly 1800 km, while it reduced to about 1200 km, at 09:56 UT (see Table 1), when the clock-angle reached 90° (IMF  $B_Y \sim 20$  nT, and  $B_Z \sim 0$ ). We believe that these cusp-like auroral spots are the signature of concurrent antiparallel (or, near-antiparallel) magnetic merging ongoing in different hemispheres, with the ionospheric footprint of the northern (local) cusp displaced in the postnoon, and the magnetically conjugated footprint of the southern cusp displaced in the prenoon, due to the effect of the positive IMF  $B_Y$  component. The observed prenoon cusp-like aurora signature implies that, for an IMF clock-angle  $\geq 45^\circ$ , on the prenoon flank of the southern cusp there was the condition to have (near)antiparallel merging on magnetic field lines connected to the Northern Hemisphere (region I, Fig. 1). This condition was probably favoured by: i) the presence of a positive IMF  $B_X$  component (between 09:00–09:55 UT) that, for a non-zero IMF  $B_Y$ , is expected to widen the antiparallel merging region near the southern cusp, while shrinking the corresponding one near the northern cusp (Luhmann et al., 1984); ii) the fact that, when the IMF  $B_Y$  and the dipole tilt angle are both non zero, there is an equatorward displacement of the antiparallel merging region that is located in the summer hemisphere (presently, the southern one) (Park et al., 2006).

Trattner et al. (2005) performed a coordinated study, based on Cluster and SuperDARN data, of a double cusp structure (actually a longitudinal bifurcation) during IMF clock-angle of about 135°, finding evidences that the two cusp spots were associated to magnetic merging patches located in different hemispheres, and separated by about  $10 R_E$ .

Recently, Sandholt and Farrugia (2003), and Sandholt et al. (2004), presented some events of longitudinally bifurcated cusp aurora, during a steady south-east oriented interplanetary magnetic field ( $B_Y = 3$  nT,  $B_Z = -3$  nT,  $\theta \sim 135^\circ$ ). The main difference with the present event is that the longitudinal bifurcation we observed during northeast IMF, was likely the ionospheric signature of (near)antiparallel reconnection equatorward the dawn flank of the southern cusp (region I), and poleward the northern (local) cusp (region IV), while in the cases reported during southeast IMF, such

**Table 1.** Bifurcated cusp position and separation.

Time (UT)	West CUSP (MLAT, MLT)	East CUSP (MLAT, MLT)	Distance (km)
09:27	+72.8°, 9.13	+74.5°, 12.40	1775
09:32	+72.8°, 9.21	+74.5°, 12.48	1775
09:39	+73.6°, 9.48	+73.1°, 12.42	1610
09:43	+74.5°, 9.63	+74.5°, 12.66	1530
09:56	+75.3°, 10.47	+73.6°, 12.76	1210

bifurcation was produced by antiparallel reconnection taking place equatorward both cusps (i.e., regions I and III). Sandholt and Farrugia (2003) reported also the presence of a 500 km gap (“gap aurora”) between the two cusp spots, with dim/no emission. That value is close to the smallest separation we observed, about 550 km, when the IMF clock-angle was  $\sim 90^\circ$  (09:56 UT, lower panel of Fig. 3). Whereas, the maximum gap was nearly twice ( $\geq 1100$  km) at 09:34 UT, and 09:43 UT, with an IMF clock-angle close to 45°–50°. The extension of the gap aurora was derived by taking, as reference, the isolevel corresponding to the mean intensity of the gap aurora (about twice the background intensity). The presence of dim red emission within the gap is likely connected to a steady, even if poorly efficient, component reconnection in the subsolar region, as previously underlined by other authors (Sandholt et al., 2004). Furthermore, Fig. 3 clearly shows that such gap aurora is markedly shifted in the prenoon (by about 01:00 MLT), an aspect that is also in good agreement with the model proposed by Sandholt et al. (2004).

To inspect the conditions of the ionospheric convection during the progress of the event, we performed a preliminary survey of the SuperDARN online archive (<http://superdarn.jhuapl.edu/>). We detected the set up of sunward flow over the Svalbard, in connection with the cusp aurora emission during northward IMF ( $\approx 09:10$ – $09:30$  UT), as expected for lobe reconnection. A similar association between ionospheric sunward flow and cusp aurora, under northward IMF, was recently reported by Milan et al. (2000). As the IMF clock-angle rotated from 45° to 90°, the ionospheric convection divided into a sunward flux in the postnoon, close to the local cusp footprint, and an antisunward flux in the prenoon, in between the two spots of the bifurcated cusp aurora. Figure 4 illustrates the dayside part of the SuperDARN convection map between 09:32–09:34 UT superimposed to the ITACA<sup>2</sup> composite image at 09:33 UT. The dashed red line sketches the location of the open/closed field line boundary, drawn by using the equatorward edge of the 630.0 nm emission as a proxy. The two numbered markers indicate the location of the magnetospheric boundaries recorded by the two DMSP transits closest to the period considered (see Table 2). From this figure it can be noted that the prenoon and postnoon

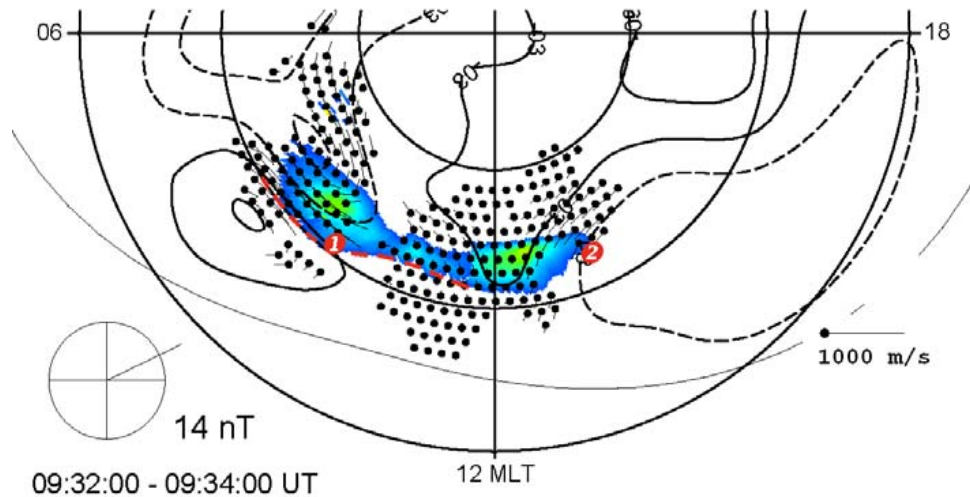


**Fig. 4.** SuperDARN ionospheric convection map between 09:32–09:34 UT, superimposed to the combined ITACA<sup>2</sup> red-line images (projected at 400 km height). The dashed red line sketches the open/closed field line boundary, drawn by taking the equatorward edge of the 630.0 nm emission as a proxy. The two numbered markers indicate the location of the magnetospheric boundaries recorded by the two DMSP transits closest to the period considered (see Table 2). The open/closed field line boundary stops near magnetic noon because the field lines are convecting sunward across the local cusp auroral spot, in the postnoon, due to the reconnection ongoing at the northern lobe (as traced by the sunward ionospheric flow). The prenoon and postnoon cusp auroras reside on separate convection cells, indicating that they are linked to different merging regions, likely located in the Southern and Northern Hemisphere, respectively (as sketched in Fig. 1). The ionospheric flow moving antisunward across the “gap” aurora, about 1 h before noon, could be the signature of component merging ongoing in the subsolar region (marked as II, in Fig. 1).

**Table 2.** Magnetospheric boundaries from DMSP data (see Fig. 4).

Time (UT)	DMSP satellite	boundary position (MLAT, MLT)	boundary type
09:12:08	F13	+71.2°, 9.6	LLBL/cusp
09:40:32/24	F15	+72.7°/73.0°, 13.5/13.6	BPS/LLBL/BPS

auroral spots clearly reside in different convection cells, indicating that they are likely connected to merging regions located in different hemispheres (southern and northern, respectively), as sketched in Fig. 1. Figure 4 shows also the antisunward ionospheric flow crossing the gap aurora in the prenoon. The development of that antisunward flow is very interesting since it supports the idea of the activation of component merging in the subsolar magnetopause in association with the gap aurora formation. This finding seems to favor the “mixed” reconnection theory with respect to the pure antiparallel reconnection view.

### 3.2 Longitudinal and latitudinal cusp bifurcation during IMF clock-angle $\sim 90^\circ$

A net discontinuity in the solar wind occurred between 09:48–09:54 UT: both IMF  $B_X$  and  $B_Z$  components turned

to zero, and the ram pressure dropped from  $\sim 24$  to  $\sim 7$  nPa. During this phase, the cusp-like auroral spots faded progressively, likely because the abrupt expansion of the magnetopause drove a significant decrease the magnetic reconnection rate. Afterward, the time interval 09:55–10:45 UT was characterized by a steady eastward IMF ( $B_Y \sim 18$  nT,  $B_Z \sim 0$  nT), apart a small deviation between 10:10–10:18 UT (see Fig. 2). Between 09:55–09:58 UT, the ITACA<sup>2</sup> monitors observed the abrupt and contemporaneous (within 30 s time resolution), activation of the two cusp patches located at  $73^\circ$ – $74^\circ$  MLAT, shown in the bottom panel of Fig. 3 (09:56 UT). At the same time, a sequence of green rayed arcs started in the high-latitude postnoon, at about  $77^\circ$  MLAT, a feature that we identified as type 2 cusp auroras. This activity had been usually reported during northward directed IMF, and associated to the ionospheric signature of lobe reconnection (e.g.: Øieroset, 1997; Sandholt et al., 1996, 1998). Figure 5, upper panel, illustrates the map projection of the day-side cusp aurora at 09:57 UT, during this activation phase. It was drawn by mapping the low-latitude 630.0 nm emission, at 400 km of altitude (as in Fig. 3), and then by adding the 630.0 nm emission associated to the high-latitude arc, projected at 200 km of altitude. To calculate the last value, we mapped the 557.7 nm green line emission (Fig. 5, lower right panel) at a reference altitude of 110 km, and then adjusted the projection altitude of the associated 630.0 nm red line emission (Fig. 5, lower left panel) until they overlapped. That

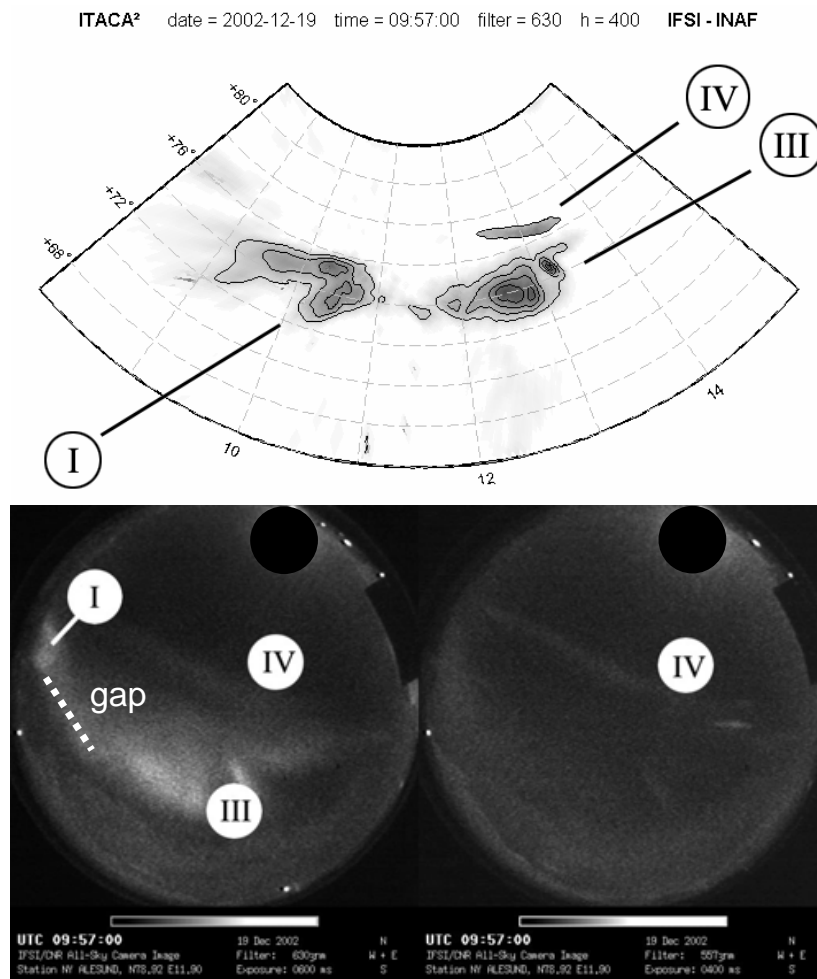


**Fig. 5.** Upper panel: MLAT versus MLT mapping projection of combined ITACA-DNB and ITACA-NAL all-sky images (630.0 nm). The estimated peak emission height is 350–400 km for patches I and III, and 200 km for patch IV. Lower panel: ITACA-NAL red- (left) and green-line (right) all-sky images.

is, we used the simple assumption that the red and green emissions were vertically aligned. The estimated value of the peak emission height ( $\sim 200$  km) implies electron energies in the range  $\approx 0.6$ – $1.0$  keV (Millward et al., 1999), about five times higher than the one causing the red aurora emission at 400 km. The upper panel of Fig. 5 clearly shows the simultaneous occurrence of the longitudinal and latitudinal bifurcations of the cusp aurora emission. The three aurora patches are labeled according to the magnetic merging regions illustrated in Fig. 1:

- patch III (type 1 cusp aurora) corresponds to the antiparallel merging equatorward the northern cusp, shifted in the postnoon between 12:00–13:00 MLT;
- patch I (type 1 cusp aurora) is the magnetically conjugated signature of the antiparallel merging region equatorward the southern cusp, shifted in the prenoon between 10:00–11:00 MLT;
- patch IV (type 2 cusp aurora) marks the high-latitude antiparallel merging region, which is due to magnetic reconnection ongoing at the northern lobe, centered at about 13:00 MLT.

The gap (dashed line, lower left panel) corresponds to the component merging region II, located in the prenoon subsolar region (about 11:00–12:00 MLT). It is worth noting that now, with the IMF clock-angle turned to  $90^\circ$ , the longitudinal cusp bifurcation appears to be associated to the merging regions I and III, as in the events reported by Sandholt and coworkers, during southeast IMF. The latitudinal separation between red aurora emission linked to regions III and IV, was about 270–280 km ( $\sim 3^\circ$  MLAT) at its maximum extension (09:57 UT), that is, about 3–4 times smaller than the longitudinal separation between patches I and III ( $\sim 1000$  km). The latitudinal bifurcation continued to be clearly observable all along the period 09:55–10:45 UT, until the IMF clock-angle remained close to  $90^\circ$ .



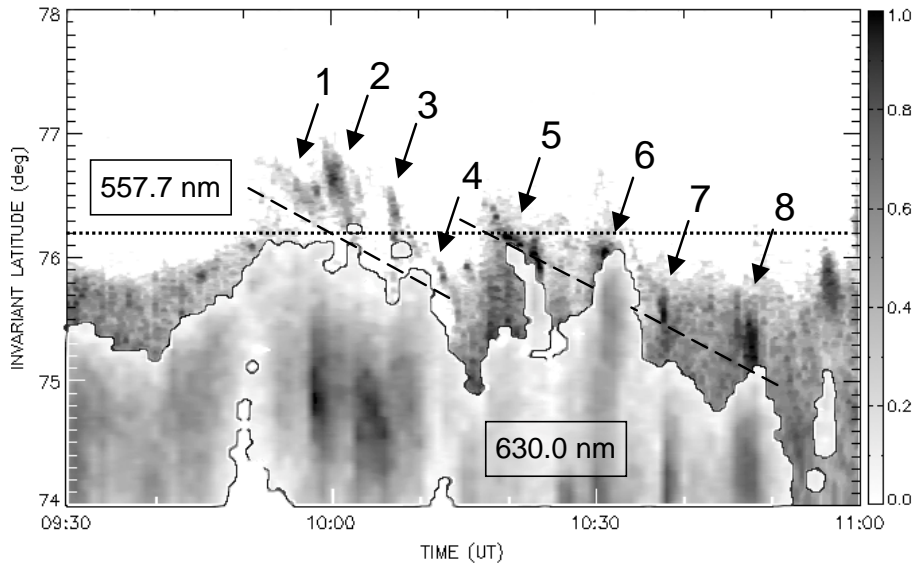


**Fig. 6.** Magnetic latitude vs. time plot of the red and green aurora emission, derived from ITACA-NAL data (intensities are in arbitrary scales). The original red and green keograms were processed to enhance the latitudinal gap between the 630.0 nm and 557.7 nm emission (indicated by two dashed lines). A peak emission height of 110 km, and 400 km, was used to calculate magnetic latitude of the green and red emission, respectively. The sequence of high-latitude type 2 cusp aurora activations (marked by arrows) developed between 09:56–10:45 UT, when the IMF clock-angle was constantly close to  $90^\circ$ . These are expected to be the ionospheric footprints of lobe reconnection events connected to the merging region IV (Fig. 1). The low-latitude type 1 cusp aurora emission, traced by the 630.0 nm emission, is the ionospheric signatures of the merging region III (Fig. 1), equatorward the local (northern cusp). The lobe reconnection footprints show a strong dependence to the IMF solar wind dynamic pressure (Fig. 2), that is: the latitude decreases as the pressure increase (about  $-0.35^\circ$  MLAT/1 nPa). A discontinuity in the solar wind dynamic pressure (see Fig. 2), caused the jump between 10:14–10:18 UT (arrows 4 and 5).

The time evolution of the latitudinal cusp bifurcation can be followed in the magnetic latitude versus time plot (keogram), shown in Fig. 6. That figure was obtained (ITACA-NAL data only) by merging the 630.0 nm keogram, which traces the low-latitude *type 1* cusp aurora (labeled as III, in Fig. 5), with the 557.7 nm keogram, which marks the high-latitude type 2 cusp aurora (labeled as IV, in Fig. 5). The original keograms were processed to improve the visualization of the latitudinal gap, roughly indicated by two dashed lines. Several intensifications of the high-latitude green arc(s) are identified by numbered arrows. By a comparison between Figs. 6 and 2 (please, note that the x-axis range is different in the two figures), we can see how the solar wind conditions affect the high-latitude auroral displacement. The latitude of the green arcs was strongly linked to the increase of the solar wind dynamic pressure (being IMF  $B_X$ ,  $B_Y$  and  $B_Z$  nearly constant), by progressively drifting from about  $77.0^\circ$  to  $75.0^\circ$  MLAT, between 09:55–10:09 UT (arrows 1–4), and from about  $76.5^\circ$  to  $75^\circ$  MLAT, between 10:19–10:45 UT (arrows 5–8). This means an average displacement of  $-0.35$  MLAT/nPa, for the ionospheric footprint of the lobe reconnection(s). The broad low-latitude red-dominated aurora (630.0 nm) showed a similar, but less extended, displacement. Between 10:09–10:18 UT, a discontinuity in the interplanetary medium, marked by a drop of the

solar wind dynamic pressure, and by the deep negative turning of the IMF  $B_X$  component, caused the green arc to break into patchy emission. Then, it reappeared few minutes after (10:19 UT), at higher latitudes, when the IMF recovered its previous orientation.

Figures 5 and 6 show that, during  $B_Y$ -dominated periods, the extent of the ionospheric footprint of merging region IV is much smaller (particularly in latitude) than the one of merging regions I, and III, and that its location is highly affected by variations in the solar wind dynamic pressure (Fig. 6). This indicates that, when  $\theta \approx 90^\circ$ , the antiparallel reconnection at the lobe, poleward the cusp, can take places only within a narrow area at the magnetopause. Conversely, the peak energy of the injected electrons is higher (0.6–1.0 keV) for the lobe merging, than for the merging equatorward the cusp (0.1–0.2 keV), resulting in a higher 557.7/630.0 intensity ratio.

### 3.3 Dynamics of antiparallel merging regions, during horizontal IMF

During the whole period dominated by horizontal IMF ( $\approx 09:55$ – $10:45$  UT), the three dayside aurora signatures labelled with I, III and IV (Fig. 5), exhibited recurrent activations followed by a net east-west (that is, tailward)

displacement, in response to the strong magnetic tension exerted by the highly positive IMF  $B_Y$  component. In particular, both the low-latitude type 1 cusp aurora patches, linked to the merging regions I and III, became very active displaying quasi-periodic emersion of new auroral forms: the patches coming from the merging region III (postnoon) overlapped with the ones originating from region I (prenoon), as both moved westward along a broad longitudinal belt ( $\approx 09:00$ – $14:00$  MLT, and  $\approx 73^\circ$ – $75^\circ$  MLAT). This aspect of the auroral activity was recently analyzed by the author, in correlation with the development of ground ULF Pc5 magnetic pulsations, shaped as a train of travelling convection vortices (TCVs) over the Greenland, close to the prenoon convection reversal boundary (CRB) (Massetti, 2005). The prenoon cusp branch, the one connected to the merging region I (Southern Hemisphere), was found to be located at/near the nose of the CRB, likely the place where the TCVs originated. Clauer (2002) reported similar ULF Pc5 events (but, with longer periodicity), developing during  $B_Y$ -dominated periods, and concluded that they were likely driven by antiparallel reconnection ongoing in the opposite hemisphere, and mapping at/near the CRB. There are several similarities between the recurrent magnetic pulsations we found in concurrence with the quasi-periodic aurora activations, and the TCV activity reported by Clauer (see Massetti, 2005), leading to the idea of a possible common origin of the two phenomena. In particular, both of them was observed to take place during a nearly horizontal IMF, a configuration that leads to the longitudinal bifurcation of the cusp, due to the simultaneous antiparallel merging in different hemispheres. This fact would imply that the specific TCV activity described by Clauer and co-workers should usually take place together with a longitudinal splitting of the cusp, assuming that a horizontal IMF always leads to such magnetospheric feature. The difference of the length of periodicity between the present TCV activity (7–8 min) and the Clauer's ones (15–35 min) could be possibly related to different reconnection regimes: “bursty”, in the case of short-period events, and “steady”, in the case of long-period events. Further studies are needed to say more about the relationship between this class of recurrent TCVs, the bifurcated cusp, and associated aurora activity, during IMF  $B_Y$ -dominated periods.

In spite of the continuous brightening and superimposition of new auroral forms, the longitudinally bifurcated cusp pattern persisted till about 10:45 UT, that is, all along the time period with an IMF clock-angle close to  $90^\circ$ . The recurrent activations involved also the high-latitude (type 2) cusp aurora, which often appeared to be synchronized with the postnoon type 1 cusp aurora (see Fig. 6), with a period of about 5–10 min. The same feature was previously reported by Sandholt et al. (2001), during a  $B_Y$ -dominated period.

The dynamics of the cusp auroras observed during large IMF  $B_Y$  clearly indicates that the associated antiparallel reconnections at the magnetopause are bursty and quasi-periodic. Since the observed ionospheric footprints map to

quite different magnetospheric regions (Fig. 1), we should conclude that the bursty and quasi-periodic merging regime can be triggered, at the same instant, over a wide fraction of the dayside magnetopause, when the appropriate conditions occur.

#### 4 Comparison between ground- and space-based observations

In the last few years, the dayside cusp aurora activity has been fruitfully analyzed thanks to the new FUV instruments on board the IMAGE Satellite (e.g. Frey et al., 2003). The good coverage of the present event allows for an interesting comparison between our ground-based twin monitors observations and the FUV satellite data. Here, we briefly focus on three cusp aurora features discussed in the Sects. 3.1 and 3.2, namely: the cusp aurora during northward IMF (09:08–09:27 UT), and the longitudinal and latitudinal cusp bifurcation signatures.

Thanks to the FUV data, it was clearly shown that, during a stable northward directed IMF, the cusp can be usually identified as a bright spot near the magnetic noon, detached from the auroral oval and poleward of it (see, for example, Fig. 2 in Fuselier et al., 2003). That spot can be observed as long as the IMF is positive, supporting the idea of a continuous reconnection under stable IMF configuration. As the IMF rotates from northward to eastward (westward) the cusp spot gradually merges with the postnoon (prenoon) dayside auroral oval, and a longitudinal gap appears aside the cusp spot in the prenoon (postnoon) sector (see, for example, Fig. 5 in Fuselier et al., 2003). This sequence corresponds to the development of a longitudinal cusp bifurcation, produced by the occurrence of antiparallel magnetic merging in different hemispheres.

Figure 7, upper panel, shows the emersion of the cusp signature some minutes after the IMF turned northward (near 09:00 UT), as described at the beginning of Sect. 3.1. The WIC, SI13, and SI12 images (from left to right, respectively) were recorded at 09:13 UT, when the clock-angle was about  $15^\circ$ . In the present case, we can note that the cusp spot practically emerged within the dayside auroral oval, at about  $74^\circ$  MLAT, not poleward of it. We believe that this is due to the high solar wind pressure ( $\sim 12$ – $14$  nPa, see Fig. 2), which is known to push the cusp region to lower latitudes (e.g.: Newell and Meng, 1992). As the IMF clock-angle rotated eastward, the cusp spot mixed with the auroral oval in the postnoon, and was no more detectable by SI12 (sensitive to proton precipitation), while it was still apparent in both WIC and SI13 images (Fig. 7, middle panel). The FUV images in the middle panel were recorded at 09:38 UT ( $\theta \sim 40^\circ$ ), during the longitudinal cusp bifurcation sequence illustrated in Fig. 3. By comparing Figs. 3 and 7 (middle panel), it can be noticed that there is no evidence in the IMAGE data of the prenoon cusp aurora signature (circle), and that,

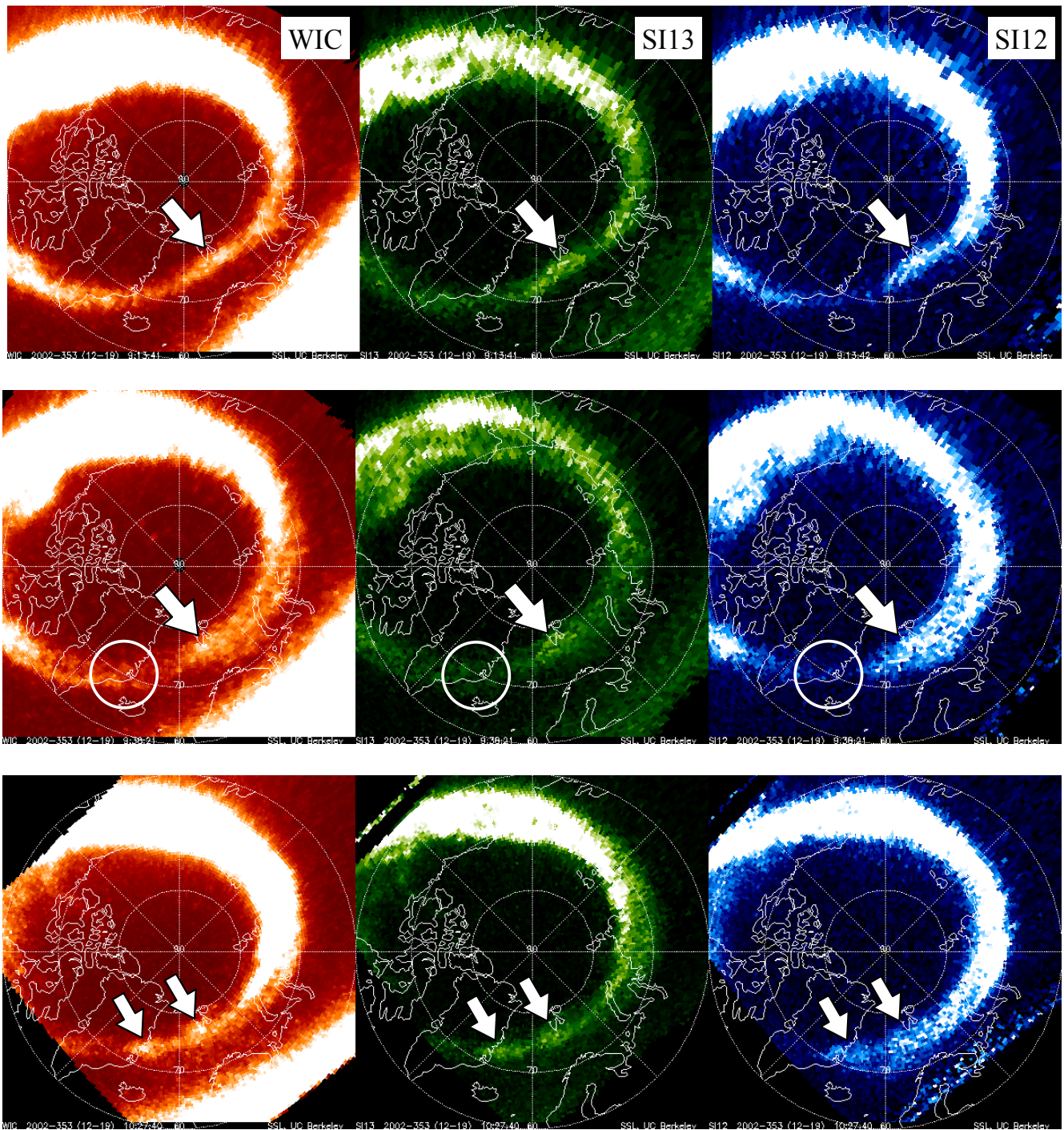


**Fig. 7.** Cusp aurora signatures as recorded by the WIC, SI13 and SI12 IMAGE-FUV instruments (from left to right). Upper panel: emersion of the cusp footprint (arrow) few minutes after the sharp IMF northward turning (09:14 UT, IMF clock-angle  $\sim 15^\circ$ ). Middle panel: cusp signature at 09:38 UT (clock-angle  $\sim 45^\circ$ ), during the longitudinal bifurcation sequence shown in Fig. 3. The circle marks the position of the (missing) prenoon cusp signature, which was observed from ground by ITACA<sup>2</sup> (Fig. 3). Lower panel: the bifurcated cusp pattern (arrows) became apparent during one of the most intense quasi-periodic re-activations (10:28 UT), occurring during the  $B_y$ -dominated phase (09:55–10:45 UT).

consequently, the longitudinal gap in the auroral emission, westward the cusp spot (white arrow), is much greater than the one observed from ground. The longitudinally bifurcated cusp pattern, and the associated activity, was in general not detectable in the IMAGE-FUV dataset, apart from some of the most intense quasi-periodic re-activations, occurred during the  $B_Y$ -dominated period (09:55–10:45 UT). The lower panel (Fig. 7) shows the FUV signatures of the prominent re-activation of both prenoon and postnoon cusp branches occurred at 10:27 UT. In the following 10–12 min, the two spots moved westward along the prenoon auroral oval, under the effect of the strong positive IMF  $B_Y$  component. Several of such tailward moving auroral forms, generally referred as PMAFs (the likely ionospheric counterparts of FTEs), were observed by ITACA<sup>2</sup> during the  $B_Y$ -dominated period, and found to be associated to a train of TCVs moving across the Greenland (Sect. 3.3).

Due to the small gap existing between of the ionospheric signatures of the latitudinal cusp bifurcation (Figs. 5 and 6), we could expect that such a feature is generally difficult to detect from space. In addition, the poleward part of such bifurcation was formed by a sequence of narrow rayed arcs (type 2 cusp aurora), drifting equatorward, which were observed to be quite dynamic. In spite of that, we found traces of such auroral activity in the WIC and SI13 images, between 09:58–10:10 UT, when the latitudinal separation was the greatest (see Fig. 6, arrows 1–3). Figure 8 reports the clearest signature we found in the WIC and SI13 images (10:07 UT). The arrow indicates the narrow and faint FUV emission corresponding to the high-latitude auroral arc, which we believe represents the ionospheric footprint of antiparallel merging region poleward the cusp, on the northern geomagnetic lobe (region IV, in Fig. 1).

## 5 Conclusions

We presented and analyzed a complex dayside auroral event, which took place near the winter solstice 2002, and was characterised by simultaneous longitudinal and latitudinal cusp bifurcations. It was recorded by ITACA<sup>2</sup>, a ground-based twin auroral monitors system, located in the high-latitude Greenland-Svalbard sector, and by the FUV instruments on board the IMAGE satellite. The event was discussed in the frame of the existing magnetic reconnection theories, using the dayside auroral activity as a proxy of the reconnection topology during IMF  $B_Y$ -dominated period. We found that the observed auroral signatures seem to agree with a “mixed” reconnection topology, constituted by a sort of superimposition of antiparallel reconnection at high latitudes and component merging in the subsolar regions (Moore et al., 2002; Sandholt et al., 2004).

The event developed during a smooth transition from northward to eastward IMF, between 09:00–09:55 UT, and then continued during a nearly steady eastward IMF, till

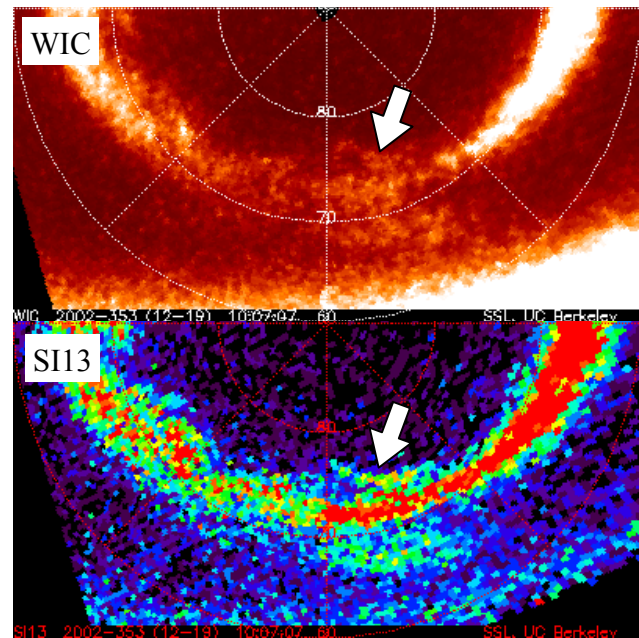


**Fig. 8.** WIC and SI13 IMAGE-FUV images recorded at 10:07 UT. The arrows indicate one of the high-latitude auroral arcs (type 2 cusp aurora) that form the poleward part of the so-called latitudinal cusp bifurcation (see Figs. 5 and 6), occurred during horizontal IMF (clock-angle  $\sim 90^\circ$ ). This auroral signature is likely the ionospheric footprint of antiparallel magnetic merging at the northern geomagnetic lobe.

about 10:45 UT. The solar wind pressure was quite high for the whole period, particularly during the first part of the event, ranging between about 24 to 7 nPa. The key features of the event are:

- i) the longitudinal cusp aurora bifurcation during north-east IMF ( $45^\circ \leq \theta \leq 90^\circ$ ),
- ii) the simultaneous longitudinal and latitudinal cusp aurora bifurcations, followed by quasi-periodic cusp aurora activations, during eastward IMF ( $\theta \simeq 90^\circ$ ).

The longitudinal cusp bifurcation is a peculiar magnetospheric-ionospheric configuration that was reported to occur during southeast/southwest IMF, clock-angle  $\sim 135^\circ$  (e.g., Sandholt et al., 2004; Trattner et al., 2005), and found to be the signature of antiparallel magnetic reconnection taking place in different hemispheres, equatorward both the northern and southern cusp, with the corresponding ionospheric footprints dislocated away from magnetic noon due to the non-zero IMF  $B_Y$  component. The event here illustrated shows that, at least during specific circumstances, the longitudinal splitting of the cusp can also take place during a northeast IMF. On the basis of the available data, we believe that this phenomenon can be explained in terms of (near)antiparallel merging occurring at the same time, poleward the northern cusp (lobe reconnection), and

equatorward the dawn flank of the southern cusp. For a non-zero IMF  $B_Y$  component, the latter condition should be favored by the presence of a positive IMF  $B_X$  component, which is expected to widen the antiparallel merging region in the Southern Hemisphere, and by the negative dipole tilt during the winter solstice, which is expected to cause an equatorward shift of the same merging region.

The ITACA<sup>2</sup> all-sky images show the simultaneous occurrence of both type 1 and type 2 cusp auroras, in three separate areas of the high-latitude ionosphere, mapping to three very distinct regions of the dayside magnetopause: two of them equatorward the northern (local) and southern cusp, and the other one poleward the local cusp, at the northern geomagnetic lobe. These cusp auroral signatures match the ionospheric footprint pattern that can be drawn by assuming antiparallel reconnection(s) ongoing at high-latitudes, during IMF  $B_Y$  dominated periods (e.g.: Moore et al., 2002; Sandholt et al., 2004). Such simultaneous occurrence of both longitudinal and latitudinal cusp aurora bifurcations was never reported before, to our knowledge.

Other relevant aspects of the event are the following:

- the simultaneous brightening of the prenoon and post-noon auroral patches of the longitudinally bifurcated cusp (09:55–09:58 UT), within 30 s time resolution. This evidence was also reported by Sandholt and Farrugia (2003) (1 min resolution), and it implies that magnetic merging events, taking place in different hemispheres, can happen virtually at the same time. When generated by the variability of the interplanetary condition, a time lag between the ionospheric signatures of reconnections in different hemispheres arises from both the dipole tilt angle and the IMF  $B_X$  (e.g., Maynard et al., 2002). In the present case, we have that the IMF  $B_X$  component was close to zero during the simultaneous activation of the bifurcated cusp, implying no delay associated to the inclination of the IMF plane. As a consequence, the potential lag due to the tilt of the Earth's magnetic dipole, which was close to its maximum (winter solstice), must be smaller than 30 s (the ITACA<sup>2</sup> time resolution). A possibility could be that the simultaneous auroral activations were triggered by the large-scale reorganization of the dayside magnetosphere occurred after the drop of the solar wind pressure (24→7 nPa, between 09:48–09:54 UT), which was accompanied by an IMF clock-angle rotation to 90°;
- the existence of a dim red emission in between the gap separating the longitudinal bifurcated cusp. That feature should be associated with a steady, low-efficient, component reconnection ongoing on the subsolar region, as depicted by the “mixed” merging model (Sandholt et al., 2004). This idea is supported by the evidence we found of an antisunward ionospheric flow through the gap aurora (Sect. 3.1). The gap aurora was visibly shifted in the prenoon, by about 01:00 MLT, again in agreement

with previous observations and with the model proposed by Sandholt et al. (2004);

- thanks to the wide field-of-view of the ITACA<sup>2</sup> twin monitors, it was possible to make a large-scale comparison with the IMAGE-FUV data. The comparison shows relevant differences between ground- and space-based observations of the same cusp aurora event, stressing the importance to perform coordinated studies involving both kinds of dataset. Finally, we found clear signatures of the latitudinal cusp splitting, and of the quasi-periodic aurora activations that followed the longitudinal bifurcation of the cusp, which could be the first report of such auroral activity detected in the IMAGE-FUV data.

*Acknowledgements.* The NASA Goddard Space Flight Center, L. A. Frank (CPI), and S. Kokubun (MGF), are acknowledged for the GEOTAIL satellite data. The FUV team at UC Berkeley is acknowledged for providing the IMAGE-FUV. The SuperDARN team is acknowledged for providing online access to several data products. The author thanks E. Amata and I. Coco for the SuperDARN ionospheric convection map reported in Fig. 4. POLARNET (IIA-CNR) is acknowledged for logistical support in running the ITACANAL station. PNRA is acknowledged for founding the ITACA<sup>2</sup> stations (PEA2002–2003, PEA2004–2006). The author acknowledges the reviewers for valuable comments and suggestions.

Topical Editor I. A. Daglis thanks H. Frey and K. Kauristie for their help in evaluating this paper.

## References

- Clauer, C. R.: Ionospheric observations of waves at the inner edge of the low latitude boundary layer, in: *Earth's Low Latitude Boundary Layer*, edited by: Newell, P. T. and Onsager, T., *Geophys. Monogr.*, 133, 297–310, 2002.
- Cowley, S. W. H.: Comments on the merging of non-parallel magnetic fields, *J. Geophys. Res.*, 81, 3455–3458, 1976.
- Cowley, S. W. H. and Owen, C. J.: A simple illustrative model of open flux tube motion over the dayside magnetosphere, *Planet. Space Sci.*, 37, 1461–1475, 1989.
- Crooker, N. U.: Dayside merging and cusp geometry, *J. Geophys. Res.*, 84, 951–959, 1979.
- Frey, H. U., Mende, S. B., Immel, T. J., Gérard, J.-C., Hubert, B., Habraken, S., Spann, J., Gladstone, G. R., Bisikalo, D. V., and Shematovich, V. I.: Summary of quantitative interpretation of IMAGE far ultraviolet auroral data, *Space Sci. Rev.*, 109, 255–283, 2003.
- Fuselier, S. A., Mende, S. B., Moore, T. E., Frey, H. U., Petrinc, S. M., Claffin, E. S., and Collier, M. R.: Cusp dynamics and ionospheric outflow, *Space Sci. Rev.*, 109, 285–312, 2003.
- Gosling, J. T., Asbridge, J. R., Bame, S. J., Feldman, W. C., Paschmann, G., Sckopke, N., and Russell, C. T.: Evidence for quasi stationary reconnection at the dayside magnetopause, *J. Geophys. Res.*, 87, 2147–2158, 1982.
- Gosling, J. T., Thomsen, M. F., Bame, S. J., Elphic, R. C. and Russell, C. T.: Plasma flow reversal at the dayside magnetopause and

- the origin of asymmetric polar cap convection, *J. Geophys. Res.*, 95, 8073–8084, 1990.
- Lockwood M., Carlson Jr., H. C., and Sandholt, P. E.: Implications of the altitude of transient 630-nm dayside auroral emission, *J. Geophys. Res.*, 98, 15 571–15 588, doi:10.1029/93JA00811, 1993.
- Lockwood M., McCrea, I. W., Milan, S. E., Moen, J., Cerisier, J. C., and Thorolfsson, A.: Plasma structure within poleward-moving cusp/cleft auroral transient: EISCAT Svalbard radar observations and an explanation in terms of large local time extent of events, *Ann. Geophys.*, 18, 1027–1042, 2000, <http://www.ann-geophys.net/18/1027/2000/>.
- Luhmann, J. G., Walker, R. J., Russell, C. T., Crooker, N. U., Spreiter, J. R., and Stahara, S. S.: Patterns of potential magnetic field merging sites on the dayside magnetopause, *J. Geophys. Res.*, 89, 1739–1742, 1984.
- Massetti, S.: Dayside magnetosphere-ionosphere coupling during IMF clock-angle  $\sim 90^\circ$ : longitudinal cusp bifurcation, quasi-periodic cusp-like auroras and traveling convection vortices, *J. Geophys. Res.*, 110, A07304, doi:10.1029/2004JA010965, 2005.
- Maynard, N. C., Bruke, W. J., Moen, J., Sandholt, P. E., Lester, M., Ober, D. M., Weimer, D. R., and White, W. W.: Bifurcation of the cusp: Implications for understanding boundary layers, in: Earth's Low Latitude Boundary Layer, edited by: Newell, P. T. and Onsager, T., *Geophys. Monogr.*, 133, 319–328, 2002.
- McCrea, I. W., Lockwood, M., Moen, J., Pitout, F., Eglitis, P., Aylward, A. D., Cerisier, J.-C., Thorolfsson, A., Milan, S. E.: ESR and EISCAT observations of the response of the cusp and cleft to IMF orientation changes, *Ann. Geophys.*, 18, 1009–1026, 2000, <http://www.ann-geophys.net/18/1009/2000/>.
- Milan, S. E., Lester, M., Cowley, S. W. H., and Brittnacher, M.: Dayside convection and auroral morphology during an interval of northward interplanetary field, *Ann. Geophys.*, 18, 436–444, 2000, <http://www.ann-geophys.net/18/436/2000/>.
- Millward, G. H., Moffett, R. J., Balmforth, H. F., and Rodger, A. S.: Modeling the ionospheric effects of ion and electron precipitation in the cusp, *J. Geophys. Res.*, 104, 24 603–24 612, doi:10.1029/1999JA900249, 1999.
- Moore, T. E., Fok, M.-C., and Chandler, M. O.: The day-side reconnection X line, *J. Geophys. Res.*, 107, 1332, doi:10.1029/2002JA009381, 2002.
- Němeček, Z., Šafránková, J., Přeč, L., Šimunek, J., Sauvaud, J.-A., Fedorov, A., Stenuit, H., Fuselier, S. A., Savin, S., Zelenyi, L., and Berchem, J.: Structure of the outer cusp and sources of the cusp precipitation during intervals of a horizontal IMF, *J. Geophys. Res.*, 108, 1420, doi:10.1029/2003JA009916, 2003.
- Newell, P. T. and Meng, C.-I.: Mapping the dayside ionosphere to the magnetosphere according to the particle precipitation characteristics, *Geophys. Res. Lett.*, 19, 609–612, 1992.
- Øieroset, M., Sandholt, P. E., Denig, W. F., and Cowley, S. W. H.: Northward interplanetary magnetic field cusp aurora and high-latitude magnetopause reconnection, *J. Geophys. Res.*, 102, 11 349–11 362, doi:10.1029/97JA00559, 1997.
- Park, K. S., Ogino, T., and Walker, R. J.: On the importance of antiparallel reconnection when the dipole tilt and IMF  $B_Y$  are nonzero, *J. Geophys. Res.*, 111, A05202, doi:10.1029/2004JA010972, 2006.
- Phan, T.-D. and Paschmann, G.: Low-latitude dayside magnetopause and boundary layer for high magnetic shear I. Structure and motion, *J. Geophys. Res.*, 101, 7801–7816, 1996.
- Sandholt, P. E., Farrugia, C. J., Øieroset, M., Stauning, P., and Cowley, S. W. H.: Auroral signature of lobe reconnection, *Geophys. Res. Lett.*, 23, 1725–1728, doi:10.1029/96GL01846, 1996.
- Sandholt, P. E., Farrugia, C. J., Moen, J., Noraberg, Ø., Lybekk, B., Sten, T., and Hansen, T.: A classification of dayside auroral forms and activities as a function of interplanetary magnetic field orientation, *J. Geophys. Res.*, 103, 23 325–23 346, doi:10.1029/98JA02156, 1998.
- Sandholt, P. E., Farrugia, C. J., Cowley, S. W. H., Lester, M., Denig, W. F., Cerisier, J. -C., Milan, S. E., Moen, J., Trondsen, E., and Lybekk, B.: Dynamic cusp aurora and associated pulsed reverse convection during northward interplanetary magnetic field, *J. Geophys. Res.*, 105, 12 869–12 894, doi:10.1029/2000JA900025, 2000.
- Sandholt, P. E., Farrugia, C. J., Cowley, S. W. H., and Lester, M.: Dayside auroral bifurcation sequence during  $B_Y$ -dominated interplanetary magnetic field: Relationship with merging and lobe convection cells, *J. Geophys. Res.*, 106, 15 429–15 444, doi:10.1029/2000JA900161, 2001.
- Sandholt, P. E. and Farrugia, C. J.: Does the aurora provide evidence for the occurrence of antiparallel magnetopause reconnection?, *J. Geophys. Res.*, 108, 1466, doi:10.1029/2003JA010066, 2003.
- Sandholt, P. E., Farrugia, C. J., and Denig, W. F.: Detailed day-side auroral morphology as a function of local time for southeast IMF orientation: implications for solar wind-magnetosphere coupling, *Ann. Geophys.*, 22, 3537–3560, 2004, <http://www.ann-geophys.net/22/3537/2004/>.
- Trattner, K. J., Fuselier, S. A., Petrinc, S. M., Yeoman, T. K., Mouikis, C., Kucharek, H., and Reme, H.: Reconnection sites of spatial cusp structures, *J. Geophys. Res.*, 110, A04207, doi:10.1029/204JA010722, 2005.